
THERMAL METHODS

Infrared Thermographic Testing of Hybrid Materials Using High-Power Ultrasonic Stimulation

D. A. Derusova^{a, *}, V. P. Vavilov^a, Guo Xingwang^b, V. Yu. Shpil'noi^a, and N. S. Danilin^c

^aTomsk Polytechnic University, Tomsk, 634028 Russia

^bSchool of Mechanical Engineering and Automation, Beihang University, Haidian District, Beijing, 100191 China

^cZAO Roskosmos, Moscow, 107996 Russia

*e-mail: red_moon@list.ru

Received August 9, 2018

Abstract—Ultrasonic infrared thermography is a rapid and informative method of nondestructive testing, used to inspect materials and products in aviation and rocket and space industries. High-power piezoelectric emitters stimulate various materials by ultrasound and help revealing hidden flaws by local temperature changes, which can amount to tens of degrees. The possibility of optimizing the procedure of ultrasonic infrared thermography by choosing the frequency of acoustic waves so as to match the frequencies of local resonances of defects of different sizes has been investigated.

Keywords: ultrasonic infrared thermography, nondestructive testing, local defect resonance, composite materials

DOI: 10.1134/S1061830918100029

INTRODUCTION

The classical ultrasonic infrared (IR) thermography, using high-power ultrasonic stimulation, has proved successful in the detection of surface and subsurface cracks, delaminations, lacks of fusion, foreign inclusions, impact damages, and similar defects in metals, polymers, and composites [1]. Its advantages include selectivity (a defect-free material does not change its temperature) and high productivity of testing, with the main drawback being the likelihood of damaging the tested material at the sites of high-power ultrasound input, especially when it comes to magnetostrictive transducers. Nevertheless, ultrasonic infrared thermography often still makes use of powerful piezoelectric transducers (PETs) borrowed from ultrasonic welding equipment. The piezoactive components of a PET convert electric oscillations into mechanical ones and then transmit the signal to passive resonant elements of the system to raise the amplitude to the required level and to match the generator—piezoelectric-transducer system with the load. Resonant piezoelectric transducers have a narrow band of operating frequencies with small deviations from the fundamental frequency; such PETs cannot, therefore, be used for studying materials over a wide-band frequency range [2]. Resonant PETs are designed so as to achieve high acoustic power for the emitter operating at the resonance frequency and its harmonics, thereby ensuring a temperature response of the defect sufficient for its reliable identification. Thus, the informative value and express nature of this method of nondestructive testing (NDT) is due to the relatively high power of introduced ultrasound.

The use of resonant transducers in ultrasonic infrared thermography is limited by their peculiar spectral characteristics, with the acoustic energy introduced into the tested material and the efficiency of heat generation in defect area, therefore, depending on whether the frequency of the acoustic signal supplied to a radiator corresponds to its resonance frequency. At the same time, studies of the phenomenon of local defect resonance (LDR) showed that the power of heat generation in defects depends not only on the power of input acoustic signal, but also on whether the acoustic carrier frequency corresponds to the frequency of local resonance [3–5]. Hence it follows that for effective detection of defects, it is necessary to first determine their resonance frequency. This can be done with a relatively laborious and expensive method of laser vibrometry, which is hardly applicable to the NDT of ready-made devices and articles. An alternative to this approach is to use high-power PETs, but in any event, it is of academic interest to examine how critical the correspondence between acoustic and local-resonance frequencies is. The present paper is concerned with this analysis.

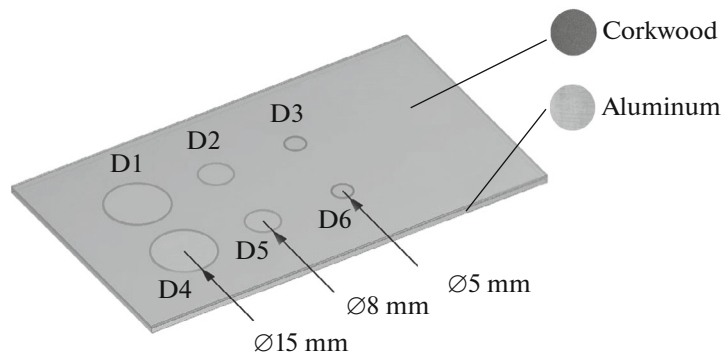


Fig. 1. Configuration of hybrid duralumin–cork-compound sample weakened by flat-bottom holes.

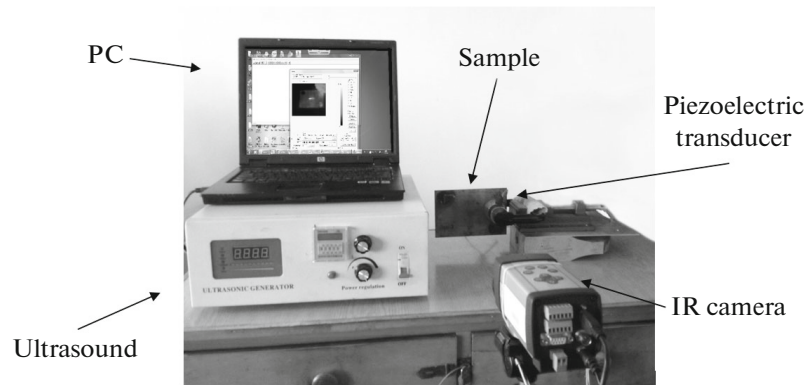


Fig. 2. Experimental setup for ultrasonic infrared thermography based on resonant piezoelectric transducer (Beihang University, China).

1. MATERIALS AND METHODS

It makes sense to study interaction between defects and elastic mechanical waves using samples that contain some reference defects, for example, in the form of cylindrical recesses of material at the back surface of the sample (flat-bottom holes). Despite the simple geometrical shape, such defects in some cases rather accurately model situations encountered in practice and are often applied in other NDT methods. In our studies, the reference sample was a rectangular duralumin plate ($200 \times 120 \times 2.7$ mm) glued together with a plate of crushed cork compound with a thickness of 1 mm. The hybrid sample contained six defects in the form of cylindrical holes with diameters $\varnothing 15$ (D1 and D4), 8 (D2 and D5), and 5 (D3 and D6) mm (Fig. 1). Note that in this case the cork layer imitates heat protection used in rocket and space engineering products.

Experiments were carried out using the ultrasonic IR thermography facility based on resonant PET, developed at the University of Beihang, China (Fig. 2). It uses an acoustic oscillator (frequency range 15–80 kHz) that transmits the signal to one of the three available piezoelectric transducers (21.5, 26, and 41 kHz) with a rated electric power of 50 W. The reference sample was acoustically stimulated from the side of the cork layer, and its temperature was measured using an FLIR A325SC IR camera (spectral range 7.5–13 μm , temperature resolution 80 mK, IR matrix 320×240). The sequences of infrared thermograms were processed digitally on a personal computer (PC) using a dedicated piece of software developed at the University of Beihang.

The entry point of acoustic signals was at the surface of the cork layer, despite its low thermal and sound conductivity and the likelihood of a damage inflicted to it. It was assumed that ultrasonic stimulation would cause heat generation due to the activation of local (tensile-compressive) vibrations of the cork layer near the flat-bottom holes (defects).

Table 1. Frequencies of the main resonance of defects in the reference sample

| Defect | D1 | D2 | D3 | D4 | D5 | D6 |
|-------------|-----|------|------|-----|------|------|
| f_0 , kHz | 7.4 | 26.1 | 66.8 | 7.4 | 26.1 | 66.8 |

2. ELEMENTS OF THE THEORY OF LOCAL RESONANCE IN DEFECTS

When analyzing acoustic vibrations, the corkwood compound layer was considered as an isotropic medium, assuming that the corkwood plate was fixed at the sites of its bonding with metal. Then, the cork layer was considered free of vibrations near the circular blind holes and clamped along the perimeter.

These boundary conditions make it possible to consider oscillations occurring near a circular blind hole as thin-plate vibrations described in Timoshenko’s theory of elasticity [6]. Thin-plate vibrations near the circular hole are accompanied by the tension-compression strains (r) [6]

$$\epsilon_r = \frac{d}{2} \frac{\partial^2 U(r)}{\partial r^2}, \tag{1}$$

where d is the thickness of the plate near the hole, r is the coordinate of the hole radius ($r = -R \dots R$), and R is the radius of the hole.

Under conditions of natural vibrations in the plate and the main resonance, the radial distribution of the plate deflection $U(r)$ in circular blind holes of radius R under dynamic excitation is determined by the relation [7]

$$U(r) = U_0 \left(1 - \frac{r^2}{R^2}\right)^2, \tag{2}$$

where U_0 is the amplitude of vibrations at the plate center.

Using the formulas for the potential W_p and kinetic W_c energy of vibrations of a rectangular plate given in [6], the fundamental resonance frequency of the defect (f_0) can be expressed in terms of the ratio of effective rigidity k_{eff} and effective mass M_{eff} of the material in this region as

$$f_0 = \sqrt{\frac{k_{\text{eff}}}{M_{\text{eff}}}} / 2\pi, \tag{3}$$

After some transformations, we arrive at the final expression of the following form for determining the resonance frequency of a circular flat-bottom hole [8]:

$$f_0 = \frac{1.6h}{a^2} \sqrt{\frac{E}{12\rho(1-\nu^2)}}, \tag{4}$$

where a is the radius of the flat-bottom hole, h is the plate thickness near the circular hole, E is Young’s modulus, ρ is the material density, and ν is Poisson’s ratio.

Table 1 lists the fundamental-resonance frequencies of the round blind holes (see Fig. 1), calculated using the relation in Eq. 4 with allowance for the particular values of the physical properties of the corkwood compound: $\rho = 0.48 \times 10^3 \text{ kg/m}^3$, $E = 3.92 \times 10^8 \text{ H/m}^2$, $\nu = 0.02$.

3. EXPERIMENTAL RESULTS

The effect that the frequency of the stimulating high-power acoustic signal has on the efficiency of detection of flaws of different sizes was experimentally studied with the aid of three resonant PETs with resonant frequencies of 21.5, 26, and 41 kHz. The reference sample was stimulated with ultrasound for 10 s using a sinewave acoustic signal generated by the PET, alternately operating in the permissible frequency ranges while recording the sequences of infrared thermograms. Dependence of the temperature signal in the defect area on the operating frequency of the transducers, given a constant electric power equal to 50 W, is presented in Table 2.

Figure 3 shows temperature-frequency spectra of the signal in defective regions using three PETs characterized by resonance frequencies of 21.5, 26, and 41 kHz.

Table 2. Experimental temperature signals measured in the defects D1–D6 area (ultrasonic IR thermography of duralumin–cork-layer sample)

| Piezoelectric transducer with resonance frequency 21.5 kHz (transducer 1) | | | | | | | | | | | | |
|---|-----|------|------|-------|-------|-------|------|------|------|------|------|----|
| f , kHz | 17 | 18 | 19 | 20 | 21 | 21.5 | 22 | 23 | 23.5 | 24 | 25 | 26 |
| ΔT_{D1} , °C | – | – | 0.63 | 0.81 | 2.14 | 4.28 | 4.3 | 2.48 | 0.98 | 1.07 | 0.77 | – |
| ΔT_{D2} , °C | – | – | – | – | 2.71 | 6.32 | 6.38 | 2.06 | 0.47 | – | – | – |
| ΔT_{D3} , °C | 0.5 | 0.74 | 1.2 | 2.8 | 2.19 | 2.64 | 1.96 | 0.93 | 0.37 | – | – | – |
| ΔT_{D4} , °C | – | – | 0.51 | 0.79 | 4.01 | 8.52 | 9.06 | 3.61 | 1.59 | 0.65 | – | – |
| ΔT_{D5} , °C | – | – | – | – | 1.69 | 3.21 | 3.47 | 0.73 | – | – | – | – |
| ΔT_{D6} , °C | – | – | 0.52 | 1.25 | 1.76 | 2.48 | 2.21 | 0.39 | – | – | – | – |
| Piezoelectric transducer with resonance frequency 26 kHz (transducer 2) | | | | | | | | | | | | |
| f , kHz | 20 | 25 | 26 | 27 | 28 | 29 | 30 | 31 | | | | |
| ΔT_{D1} , °C | – | 0.78 | 3.14 | 2.4 | 0.66 | 0.69 | – | – | | | | |
| ΔT_{D2} , °C | – | – | 0.29 | 0.35 | 0.1 | 0.34 | – | – | | | | |
| ΔT_{D3} , °C | – | – | 0.36 | 0.12 | 0.27 | 0.15 | – | – | | | | |
| ΔT_{D4} , °C | – | 1.71 | 5.09 | 4.38 | 1.06 | 0.55 | – | – | | | | |
| ΔT_{D5} , °C | – | 1.1 | 2.72 | 2.19 | 0.57 | 1.05 | 0.44 | 0.2 | | | | |
| ΔT_{D6} , °C | – | 0.26 | 1.39 | 0.76 | 0.17 | 0.48 | – | – | | | | |
| Piezoelectric transducer with resonance frequency 41 kHz (transducer 3) | | | | | | | | | | | | |
| f , kHz | 37 | 38 | 39 | 40 | 41 | 42 | 43 | 44 | 45 | | | |
| ΔT_{D1} , °C | – | – | 1.15 | 6.07 | 6.03 | 4.33 | – | – | – | | | |
| ΔT_{D2} , °C | – | 2.83 | 6.41 | 9.24 | 11.28 | 7.96 | 1.9 | – | – | | | |
| ΔT_{D3} , °C | – | – | 1.24 | 11.23 | 18.33 | 8.14 | 2.35 | 2.09 | 2.37 | | | |
| ΔT_{D4} , °C | – | – | 0.61 | 2.25 | – | 3.4 | – | – | 1.5 | | | |
| ΔT_{D5} , °C | – | – | 2.11 | 4.01 | – | 1.53 | – | – | 1.31 | | | |
| ΔT_{D6} , °C | – | – | 1.97 | 10.38 | 24.75 | 22.32 | 8.58 | 1.99 | – | | | |

It can be seen that the maximum temperature signal near the defects was provided by transducer no. 3 at the fundamental resonance frequency with a deviation of ± 500 Hz. For a more detailed analysis of plate stimulation by this PET, Fig. 4 presents the graph of the temperature response of the defects during a 10-s stimulation period and for 35 s after the generator is turned off. As can be seen from the data, the temperature signal in the area of the holes increases exponentially in the course of stimulation and begins to drop sharply after ultrasound is switched off, which indicates no heat transfer from the operating transducer to the defect areas. It should be noted that, as expected, the largest temperature signal was observed near holes D6 and D3. This can be explained by the proximity of the design value of the fundamental resonance frequency of these two holes to the resonance frequency of the transducer. In addition, a significant temperature change (up to 25°C) in the area of these holes may be due to the proximity of the defects to the ultrasound entry point.

Despite the fact that all of the blind holes were detected in the described experiments, the detectability of flaws of different sizes can be optimized by changing the frequency of acoustic vibrations, because the optimum frequency of stimulation increases with the diameter of defects. An important feature of the results obtained is that the shape of surface temperature “fingerprints” identified in the defect zones is also associated with the frequency of ultrasound. As the frequency of guided acoustic waves approaches the frequency of the fundamental resonance of a defect, vibrations in this region involve the maximum zone around the hole, consequentially leading to an increase in its temperature. In addition, an increase in ultrasound frequency activates vibrations of higher resonance harmonics in the defect area [8], thus altering the apparent shape of defects on IR thermograms. These features of ultrasonic IR thermography speak

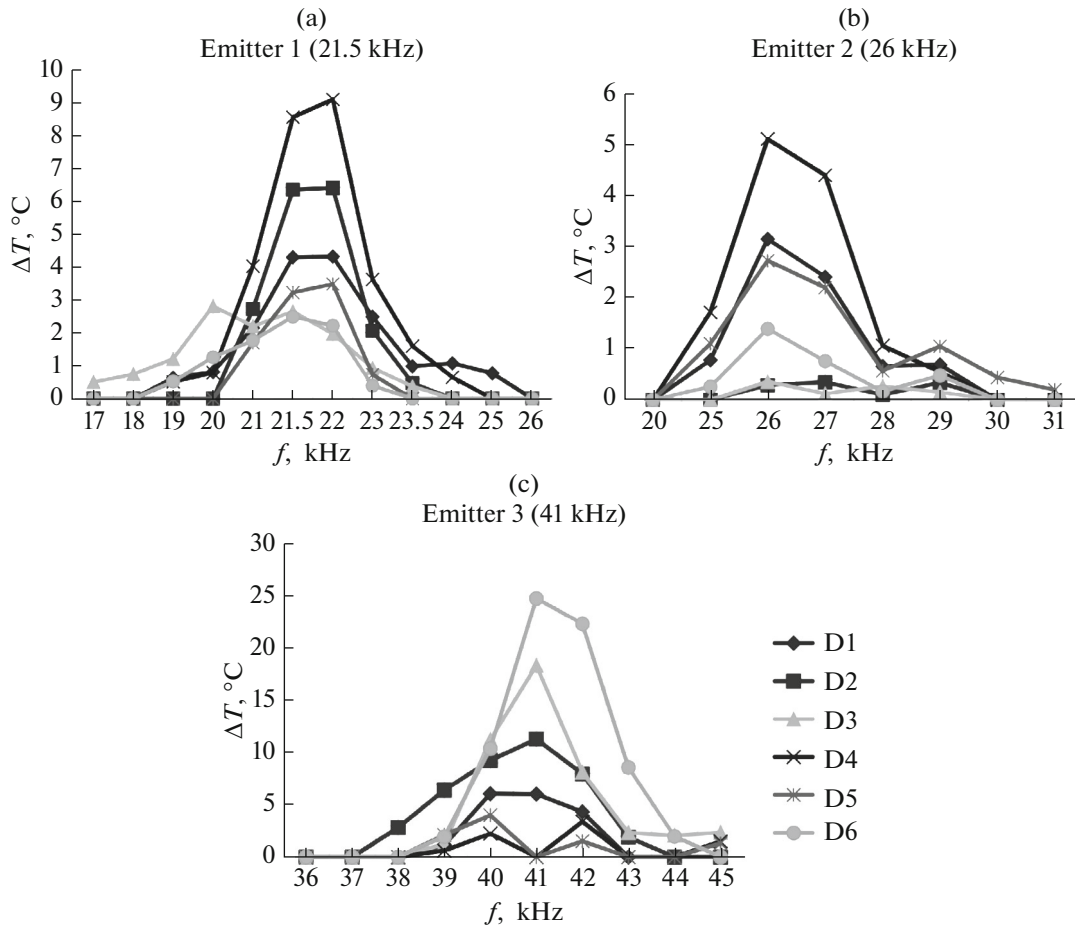


Fig. 3. Temperature-frequency spectra of signals near round holes in hybrid plate made of aluminum and corkwood compound obtained using three types of PETs.

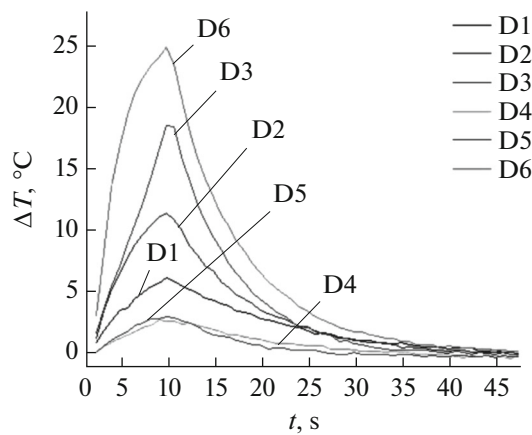


Fig. 4. Change in the temperature signal in the area of blind holes when using emitter no. 3.

in favor of using broadband ultrasonic stimulation to improve the efficiency of NDT or employing a set of resonant PETs.

Visual results of ultrasonic IR thermography for PET operating at different stimulation frequencies (within and outside the resonance region) are presented in Fig. 5. Ultrasonic stimulation of the material at the frequency of 41 kHz using transducer no. 3 additionally revealed more than 10 structural inhom-

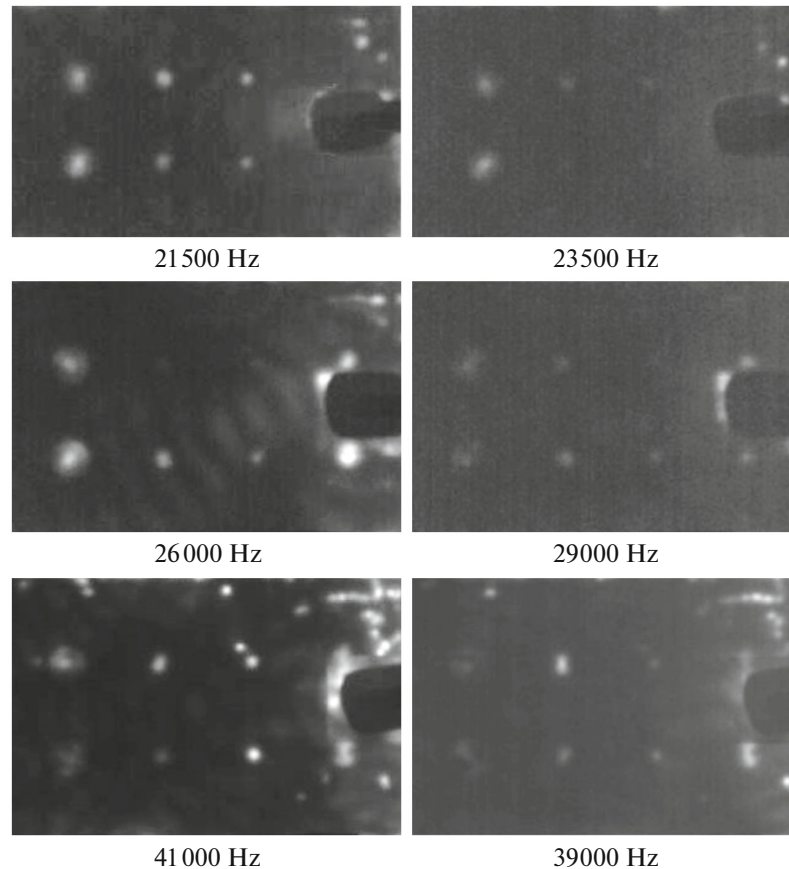


Fig. 5. Thermograms of reference sample (see Fig. 1) obtained with PET operating at resonance (21.5, 26, and 41 kHz) and out-of-resonance (23.5, 29, and 39 kHz) frequencies.

genities in the tested plate with sizes of less than 3 mm. Thus, the microinhomogeneities are detected in materials at high resonance frequencies, while for the NDT of relatively large defects it is necessary to use the PET with a low fundamental-resonance frequency.

CONCLUSIONS

IR thermography with the use of high-power ultrasound has proved itself as an informative and rapid NDT technique, allowing one to quickly (within 10–30 s) reveal structural defects of various sizes.

When detecting blind circular holes in a hybrid reference sample of duralumin and corkwood compound, it has been established that the IR-thermography shape of the surface temperature “fingerprints” essentially depends on whether the acoustic signal frequency corresponds to the frequency of defect’s fundamental resonance and its higher harmonics, changing in accordance with the shape of resonant vibrations. To better identify defect shapes, it is advisable to use broadband acoustic stimulation, which is difficult to be implemented when using resonant PETs. It has been shown that comparatively small deviations in the frequency of acoustic signal supplied to transducer (± 500 Hz and more) from the frequency of its main resonance lead to a significant decrease in the radiation intensity and a decrease in the temperature signal in the defect areas (approximately by an order of magnitude). Therefore, ensuring that the transducer operates at its own resonance frequency is a necessary condition for the effective use of ultrasonic IR thermography. In practice, this is achieved by making use of a set of resonant transducers with differing frequency characteristics.

Microinhomogeneities in materials are better detected at high resonance frequencies, while for the NDT of relatively large defects, PETs with low fundamental frequencies should be used.

ACKNOWLEDGMENTS

Introduction and Section 1 of this article were done by Guo Xingyang with the support of the grant of the National Natural Science Foundation of China no. 61571028. Sections 2, 3 and Conclusions were done at Tomsk Polytechnic University by D.A. Derusova, V.P. Vavilov, V.Yu. Shpil'noi, and N.S. Danilin and supported by Russian Science Foundation under grant no. 18-79-00029.

REFERENCES

1. Luchin, F., Dapeng, Ch., Zhi, Z., and Ning, T., Composite evaluation using contact and non-contact ultrasound excited thermography, *Appl. Mech. Mater.*, 2012, pp. 1627–1631.
2. Ermolov, I.N., Gitis, M.B., Korolev, M.V., et al., *Ul'trazvukovyye p'ezopreobrazovateli dlya nerazrushayushchego kontrolya* (Ultrasonic Piezoelectric Transducers for Nondestructive Testing), Ermolov, I.N., Ed., Moscow: Mashinostroyeniye, 1986.
3. Solodov, I., Bai, J., and Busse, G., Resonant ultrasound spectroscopy of defects: case study of flat bottomed holes, *J. Appl. Phys.*, 2013, vol.113, no. 223512.
4. Solodov, I., Döring, D., and Busse, G., Air-coupled laser vibrometry: analysis and applications, *Appl. Opt.*, 2009, vol. 48, pp. C33–C37.
5. Solodov, I., Bai, J., Bekgulyan, S., and Busse, G., A local defect resonance to enhance acoustic wave–defect interaction in ultrasonic nondestructive testing, *Appl. Phys. Lett.*, 2011., vol. 99, no. 211911.
6. Timoshenko, S.P., *Vibration Problems in Engineering*, Van Nostrand, 1956, 4th Ed.
7. Landau, L.D. and Lifshitz, E.M., *Theory of Elasticity*, vol 7: *Course of Theoretical Physics*, Butterworth-Heinemann, 1986.
8. Solodov, I., Rahammer, M., Derusova, D., and Busse, G., Highly efficient and noncontact vibrothermography via local defect resonance, *Quant. Infrared Thermogr. J.*, 2015, vol. 12(1), no. 2, pp. 98–111.

Translated by V. Potapchouck